Electronic Supplementary Material (ESI) for Physical Chemistry Chemical Physics.

Supporting information for

Investigating Molecular and Aggregated State of a Drug Molecule Rutaecarpine with Spectroscopy, Microscopy, Crystallography and Computational Studies

Shiba Sundar Dandpat and Moloy Sarkar*

School of Chemical Sciences

National Institute of Science Education and Research

Bhubaneswar 751005, India

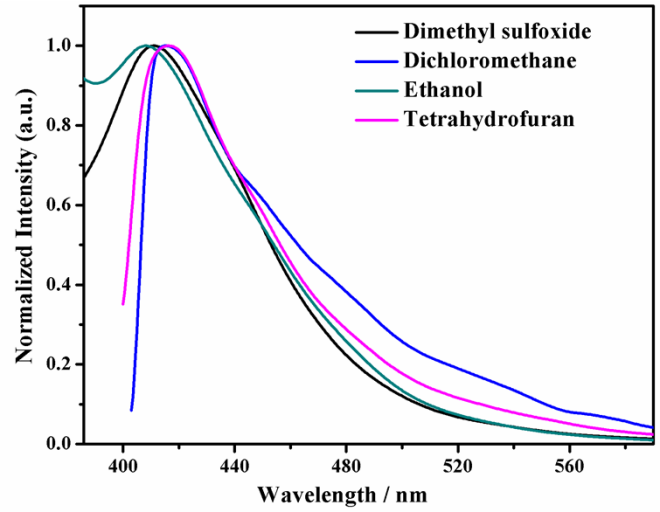

Figure S1 (a). Steady-state fluorescence profile of rutaecarpine in different solvents. λ_{ex} = 375 nm.

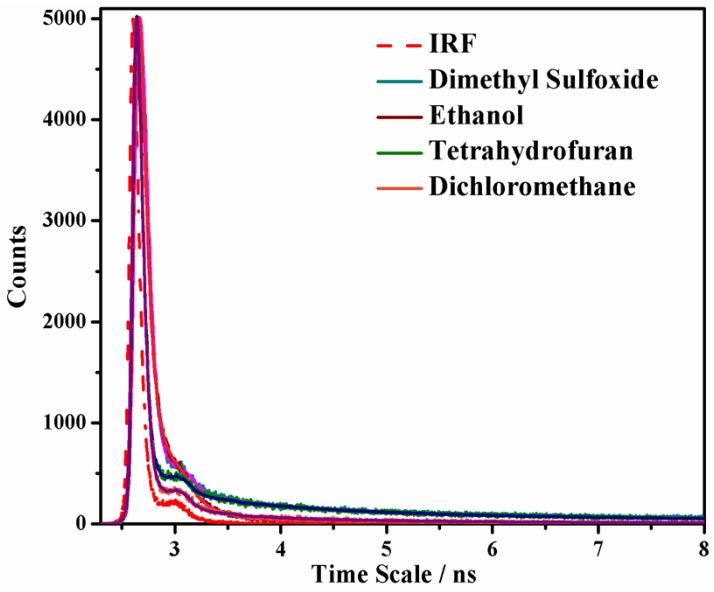

Figure S2. Time-resolved fluorescence decay profile of rutaecarpine in different solvents. λ_{ex} = 375 nm.

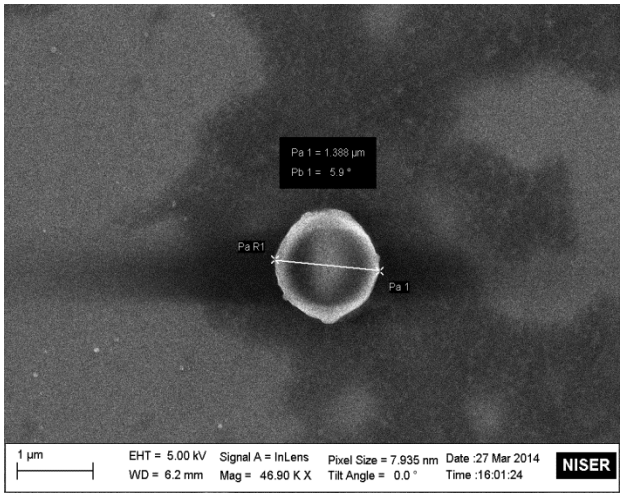

Figure S3. FESEM image of rutaecarpine colloidal aggregate with higher concentration of rutaecarpine.

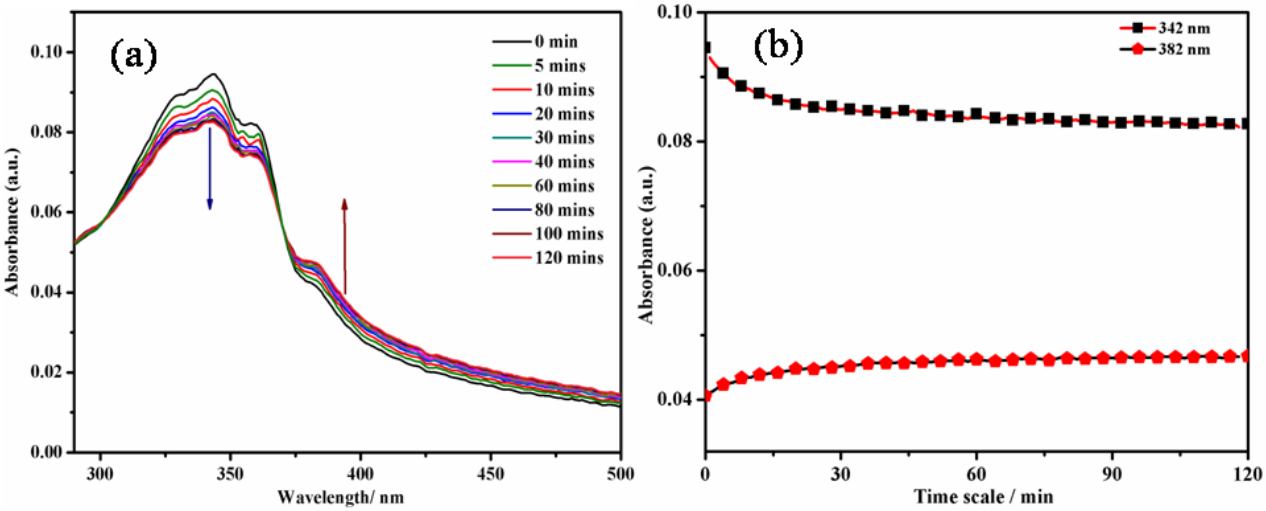

Figure S4. (a)Time dependent absorption spectra of rutaecarpine colloidal solution in water observed for 120 minutes at an interval of 10 minutes showing aging of colloids with time. (b) Variation of optical density of rutaecarpine colloidal solution with time monitored at 342 nm and 382 nm.

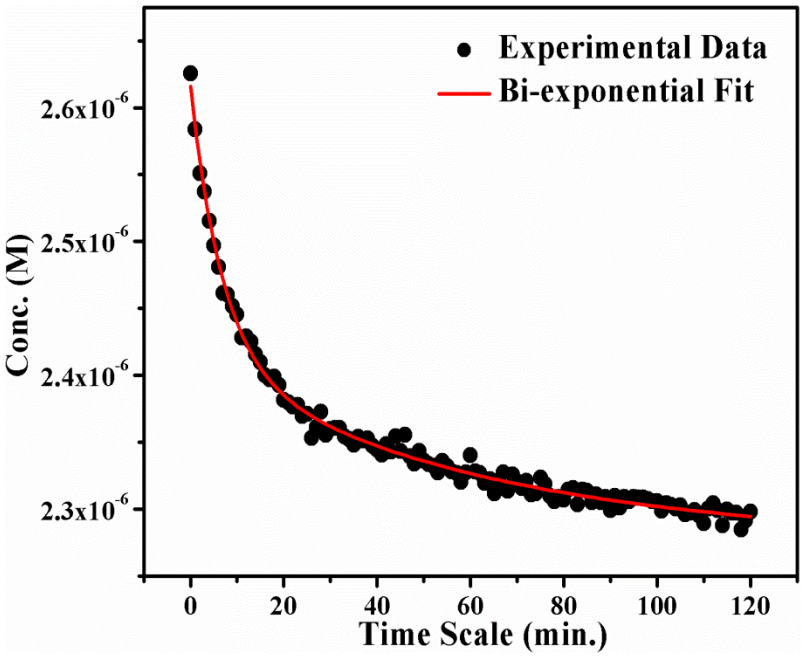

Figure S5. Time dependent variation of absorption spectrum monitored at 342 nm for colloidal solution of rutaecarpine in water

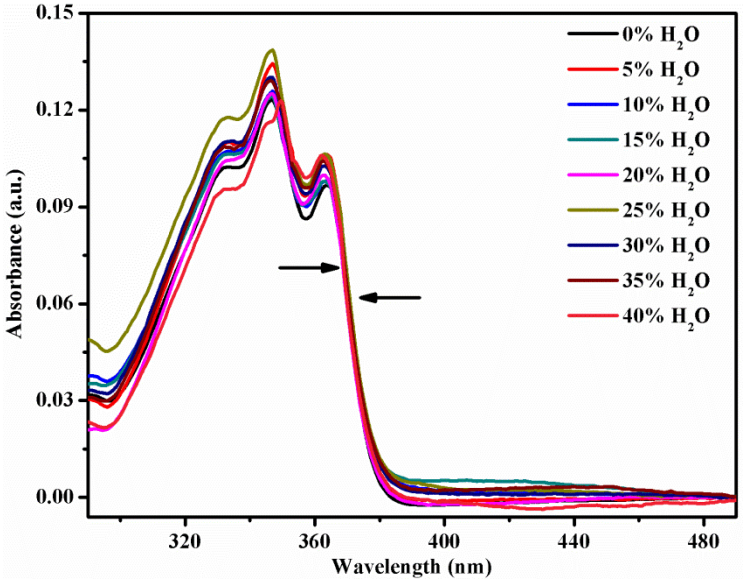

Figure S6. Absorption spectrum of rutaecarpine in DMSO with gradual increase in water content.

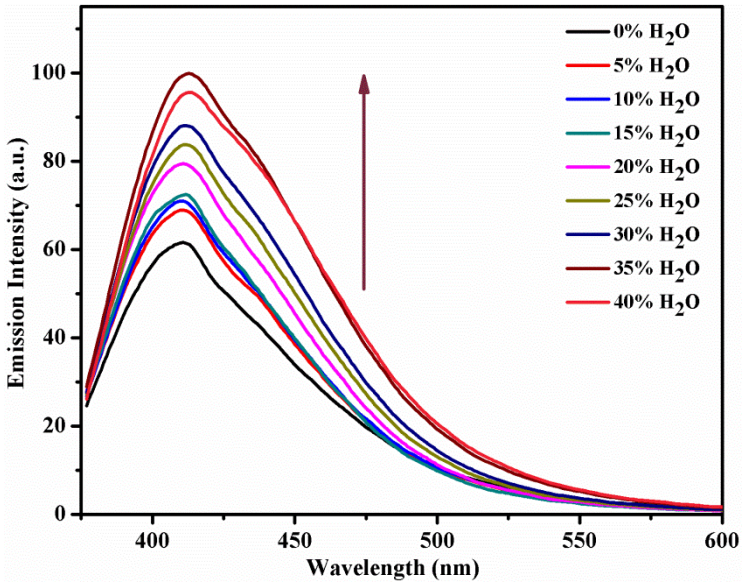

Figure S7. Steady-state emission spectrum of rutaecarpine in DMSO with gradual increase in water content. λ_{ex} = 369 nm.

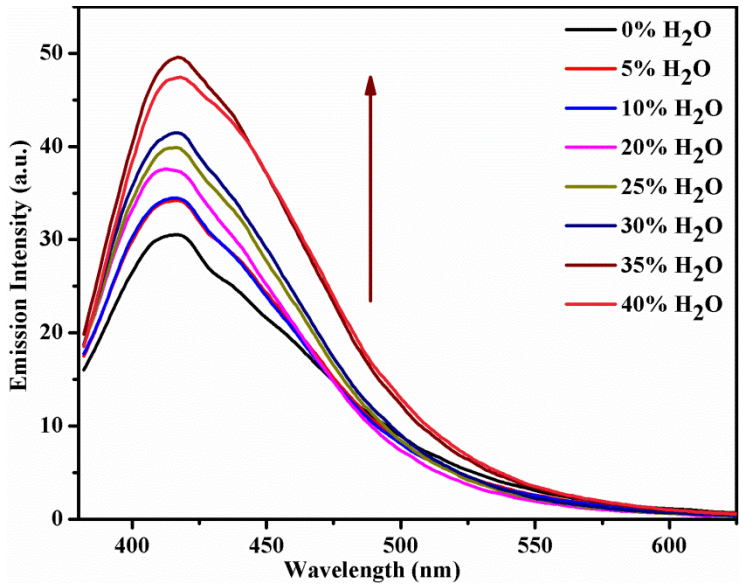

Figure S8. Steady-state emission spectrum of rutaecarpine in DMSO with gradual increase in water content. λ_{ex} = 375 nm.

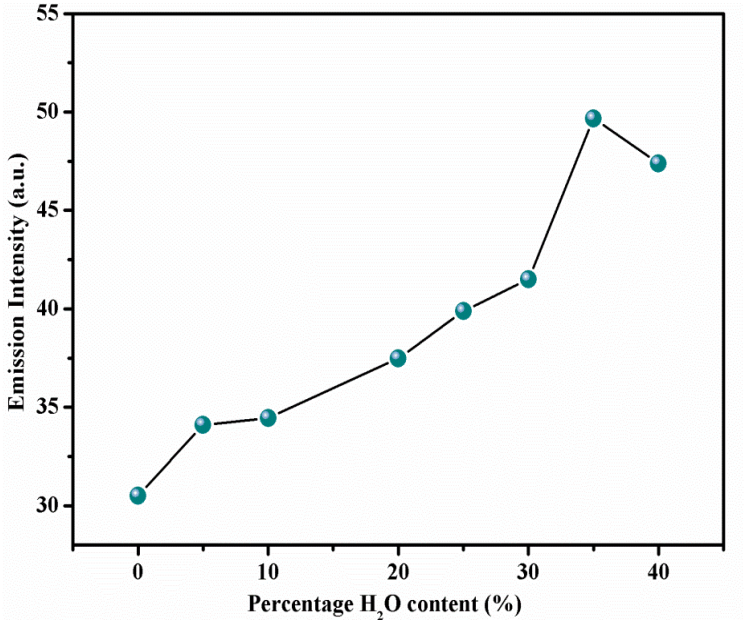

Figure S9. Variation of steady-state emission intensity of rutaecarpine in DMSO with gradual increase in water content. λ_{ex} = 375 nm.

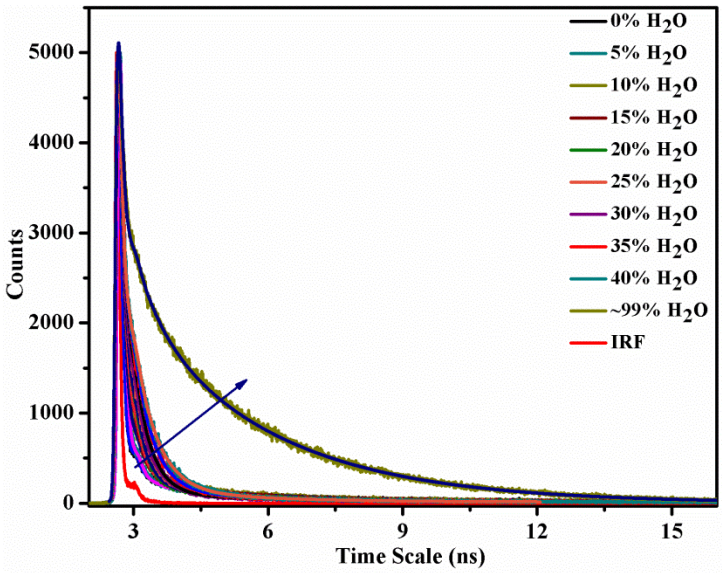

Figure S10. Time-resolved emission profile of rutaecarpine in DMSO with gradual increase in water content. λ_{ex} = 375 nm.

Table S1. Variation of time-resolved fluorescence decay components with gradual addition of water

Water Content (%)	τ_1(ps)	τ_2(ps)	τ_3(ps)	$< \tau >$ (ps)	χ^2
0	55 (0.99)	-	-	55	1.011
5	63 (0.99)	-	-	63	1.041
10	77 (0.97)	-	-	77	1.139
15	68 (0.83)	247 (0.17)	-	98	1.164
20	67 (0.78)	280 (0.22)	-	114	1.105
25	55 (0.74)	299 (0.26)	-	118	1.143
30	50 (0.75)	343 (0.25)	-	123	1.145
35	59 (0.74)	417 (0.26)	-	152	1.134
40	41 (0.80)	478 (0.20)	-	128	1.086
>98	58 (0.71)	472 (0.11)	2996 (0.18)	632	1.143

Table S2. Variation of average fluorescence lifetime of rutaecarpine colloid with temperature (K)

Temperature (K)	Average lifetime, $<\tau>$ (ps)
298	321.9
308	316.5
318	268.6
328	275.2
338	310.0
348	104.0
358	15.6

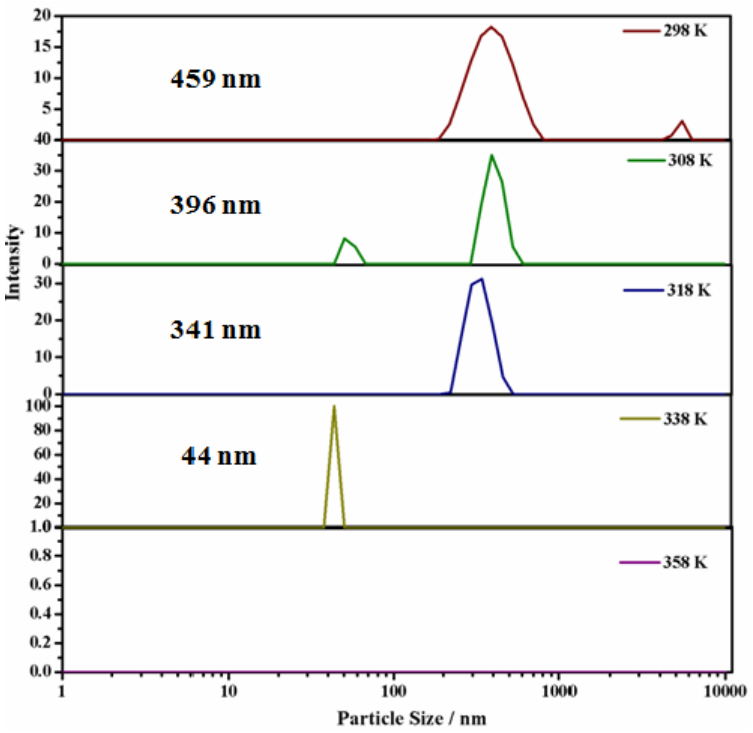

Figure S11. Variation of particle size of colloid with increasing temperature obtained through DLS measurements.

Effect of surface active ionic liquid 1-dodecyl-3-methylimidazolium bromide on optical properties of colloidal aggregate.

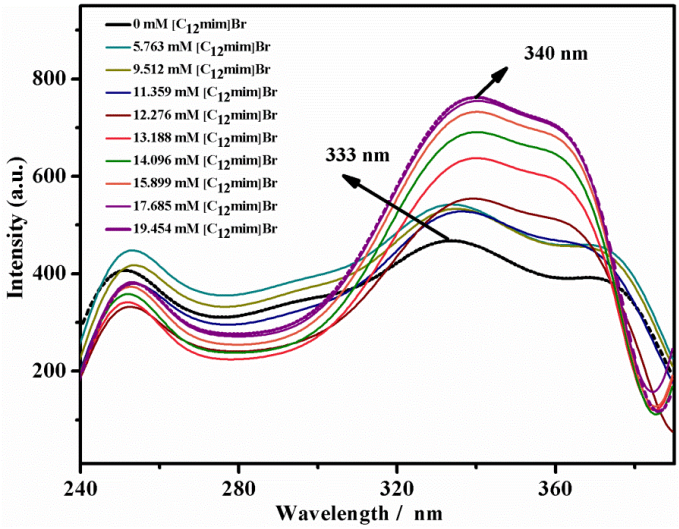

Figure S12. Variation of excitation spectra of colloidal solution of rutaecarpine with gradual addition of $[C_{12}mim]Br$.

Monitoring the excitation spectra for each emission with addition of ionic liquid (Figure S12), a flat excitation band at 333 nm was initially observed for colloidal solution which gradually shifted to 340 nm with a change in shape of spectrum showing origin for emission from different emitting species. To compare the origin of excitation bands, the excitation spectrum is recorded for monomer solution of rutaecarpine in DMSO and colloidal solution of rutaecarpine in aqueous medium showing a similar band shift from 332 nm to 340 nm (Figure S13). The excitation spectrum of colloidal solution with addition of ionic liquid to a concentration of 19.5 mM is observed to be very similar to the excitation spectra obtained for pristine solution of rutaecarpine in DMSO. This observation provides a strong evidence for degradation of colloidal aggregate towards monomer after addition of ionic liquid.

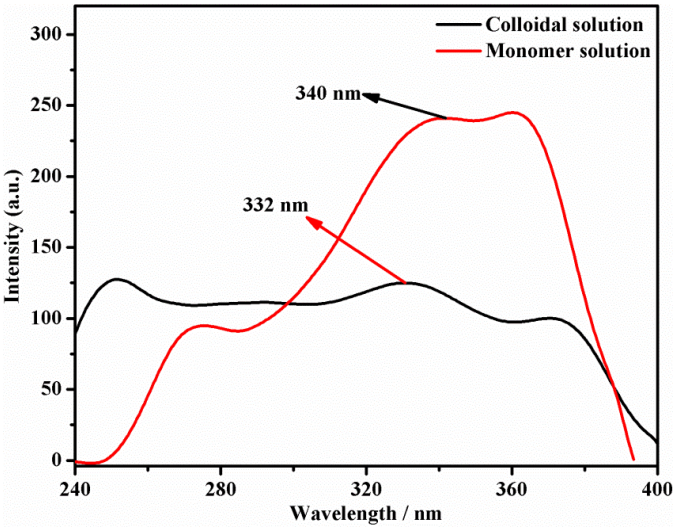

Figure S13. Excitation spectra of monomer solution of rutaecarpine in DMSO and colloidal solution of rutaecarpine.

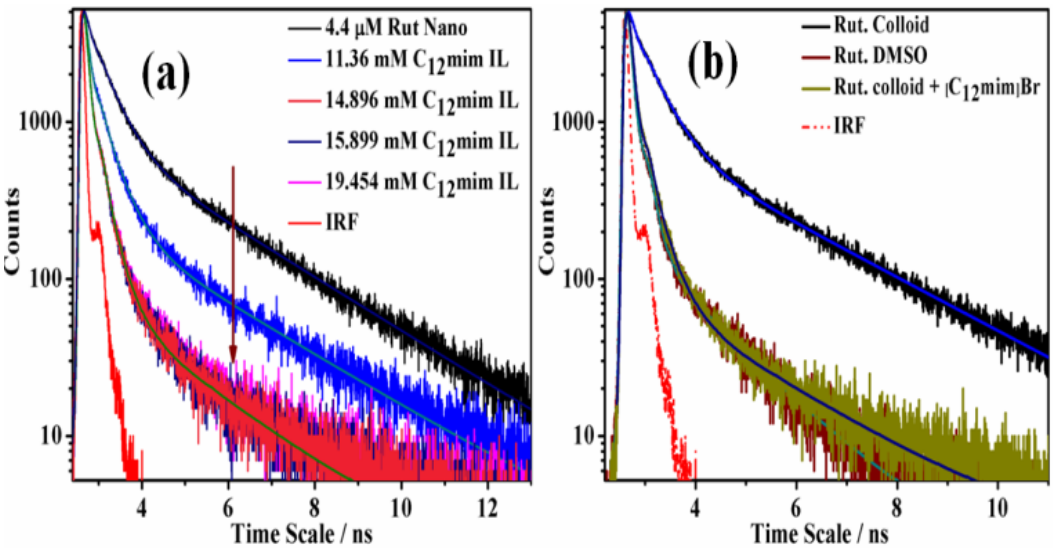

Figure S14. Variation of time-resolved fluorescence decay profile for (a) colloidal solution with gradual addition of $[C_{12}mim]Br$ ionic liquid ionic liquid (b) colloidal and monomer solution of rutaecarpine compared to colloidal solution with ionic liquid. λ_{ex} = 375 nm.

Table S3. Variation of average lifetime of rutaecarpine colloid with addition of $[C_{12}mim]Br$ ionic liquid

Conc. Of $[C_{12}mim]Br$ (mM)	**Average Lifetime, <τ>(ps)**
0	478 .0
11.36 mM	186.0
14.36 mM	87.6
17.55 mM	85.6
Rut. DMSO	54.0

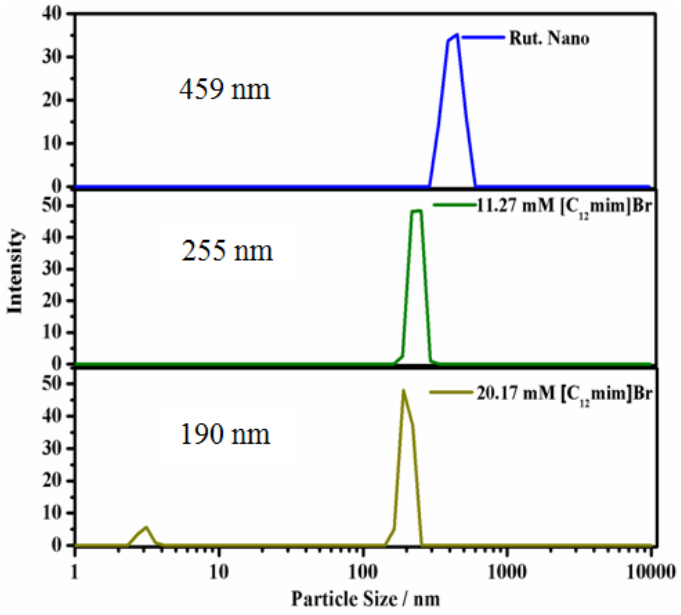

Figure S15. Variation of particle size of colloid with increasing concentration of $[C_{12}mim]Br$ ionic liquid obtained through DLS measurements.

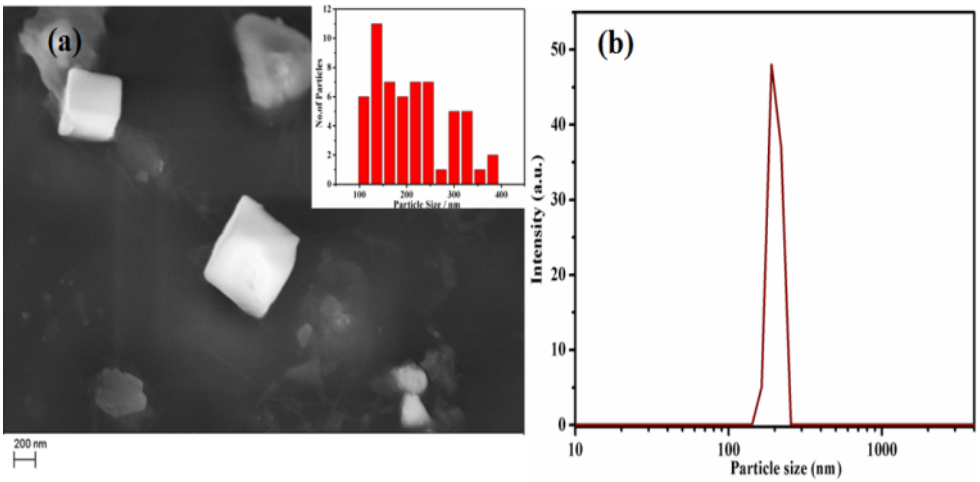

Figure S16. (a) FESEM images of rutaecarpine colloidal aggregates with 17.55 mM of $[C_{12}mim]Br$ ionic liquid showing cuboidal morphology; Inset shows particle size distribution of degraded colloidal aggregate (b) Particle size distribution plot obtained from DLS measurement.

Table S4. Types of non-covalent π-π stacked interaction in crystal packed structure of rutaecarpine (Crystal structure taken from Ref. No. 74, CCDC No. 146432)

Centroid of Monomer Unit 1	Centroid of Monomer Unit 2	π-π stacking distance (Å)
C2-C4-C6-C8-C9-C35	C1-C3-C5-C7-C10-C36	3.746
C2-C4-C6-C8-C9-C35	C10-C11-N1-C33-N5-C37	3.614
C9-C12-N2-C34-N6-C35	C10-C11-N1-C33-N5-C37	3.920
C10-C11-N1-C33-N5-C37	C9-C12-N2-C34-N6-C35	3.808
C1-C3-C5-C7-C10-C36	C9-C12-N2-C34-N6-C35	3.658
C10-C11-N1-C33-N5-C37	C2-C4-C6-C8-C9-C35	3.669

Table S5. Types of H-bonding interaction present in the 2-D crystal packing structure of rutaecarpine (Crystal structure taken from Ref. No. 74, CCDC No. 146432)

D-H…A	D-H (Å)	H…A (Å)	D…A (Å)	∠D-H…A
N3-H25…O2	0.882	2.056	2.849	149.148(102)°
N4-H26…O1	0.908	2.057	2.859	146.700(101)°

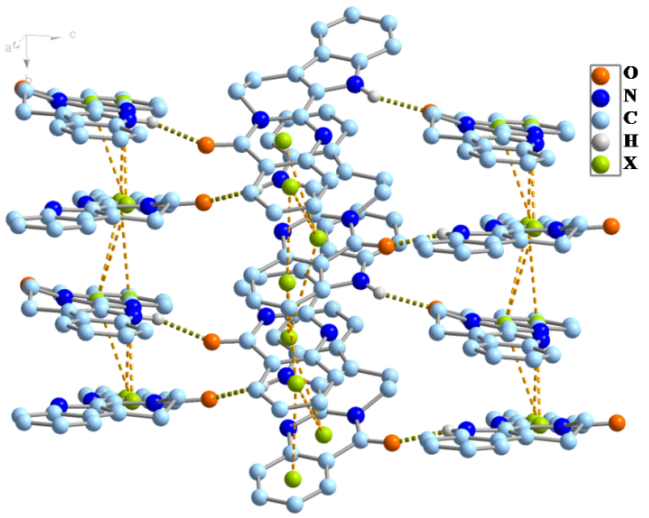

Figure S17. Three dimensional crystal packing structure of rutaecarpine showing both π-π stacked interactions (between the planes) and H-bonding interactions (between N-H…O); X representing centroid of the ring. (Crystal structure taken from ref. No. 74, CCDC No. 146432)

Table S6. Variation of absorption maxima (λ_{max}) for rutaecarpine with solvent polarization using Polarized Continuum Model (SCRF-CPCM)

Solvent	λ_{max} / nm (Oscillator Strength)	Transitions	Molar Extinction Coefficient (M^{-1} cm^{-1})
Dimethylsulfoxide (ε=46.826)	347.51(0.6969)	HOMO → LUMO	38148
	318.62 (0.3616)	HOMO-1 → LUMO	32773
Ethanol (ε= 24.852)	346.66 (0.6725)	HOMO → LUMO	37577
	318.13 (0.3635)	HOMO-1 → LUMO	32793
Dichloromethane (ε=8.93)	347.07 (0.7168)	HOMO → LUMO	38460
	318.06 (0.3242)	HOMO-1 → LUMO	32742
Tetrahydrofuran (ε=7.4257)	346.70 (0.7116)	HOMO → LUMO	38682
	317.80 (0.3184)	HOMO-1 → LUMO	32750

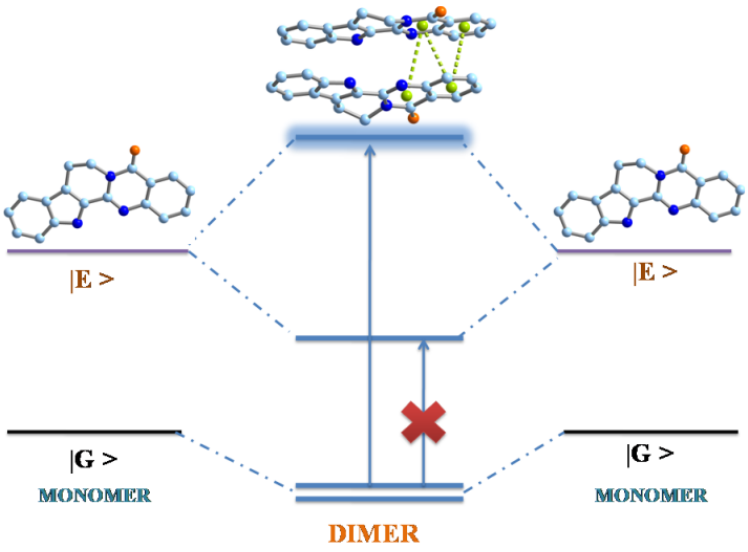

Figure S18. Exciton splitting in rutaecarpine dimer for π- π stacking arrangement of the monomers; |G> and |E> represent the wave function corresponding to ground and excited electronic states of the monomer respectively.